



## Research papers

## On operational flood forecasting system involving 1D/2D coupled hydraulic model and data assimilation

S. Barthélémy<sup>a,\*,1</sup>, S. Ricci<sup>a</sup>, T. Morel<sup>a</sup>, N. Goutal<sup>b</sup>, E. Le Pape<sup>c</sup>, F. Zaoui<sup>d</sup><sup>a</sup> CECI, CERFACS-CNRS, Toulouse, France<sup>b</sup> LHSV, EDF-R&D, Chatou, France<sup>c</sup> SCHAPI, Toulouse, France<sup>d</sup> EDF-R&D, Chatou, France

## ARTICLE INFO

This manuscript was handled by C. Corradini, Editor-in-Chief, with the assistance of Chong-Yu Xu, Associate Editor

## Keyword:

Hydraulic modeling  
Multi-dimensional coupling  
Data assimilation  
Domain decomposition  
Real time flood forecasting

## ABSTRACT

In the context of hydrodynamic modeling, the use of 2D models is adapted in areas where the flow is not mono-dimensional (confluence zones, flood plains). Nonetheless the lack of field data and the computational cost constraints limit the extensive use of 2D models for operational flood forecasting. Multi-dimensional coupling offers a solution with 1D models where the flow is mono-dimensional and with local 2D models where needed. This solution allows for the representation of complex processes in 2D models, while the simulated hydraulic state is significantly better than that of the full 1D model. In this study, coupling is implemented between three 1D sub-models and a local 2D model for a confluence on the Adour river (France). A Schwarz algorithm is implemented to guarantee the continuity of the variables at the 1D/2D interfaces while *in situ* observations are assimilated in the 1D sub-models to improve results and forecasts in operational mode as carried out by the French flood forecasting services. An implementation of the coupling and data assimilation (DA) solution with domain decomposition and task/data parallelism is proposed so that it is compatible with operational constraints. The coupling with the 2D model improves the simulated hydraulic state compared to a global 1D model, and DA improves results in 1D and 2D areas.

## 1. Introduction

The equations of fluid mechanics are solved in hydrodynamics studies with a large variety of numerical models based on simplifying assumptions. The Shallow Water equations (SWE), which are derived from the three-dimensional (3D) Navier–Stokes equations by integrating along the vertical, provide the two-dimensional (2D) simplified model of the 3D fluid flow. Subsequently, by integrating the 2D SWE across the dominant flow direction, one gets the one-dimensional (1D) SWE, also called the Saint-Venant equations. While the 1D assumption may be relevant for some rivers or sections of rivers, 2D modeling may be necessary for more complex areas such as flood plains or confluence zones. As of today, advanced hydraulic multi-dimensional modeling requires HPC (High Performance Computers). It stands in implementing robust and efficient numerical schemes over high-resolution grids together with data-driven methods such as Data Assimilation (DA) and using rich and various geophysical data (*in situ* and remote sensing). Nonetheless the lack of bathymetry/topography data and the computational cost limit the extensive use of 2D models

for operational flood forecasting. Multi-dimensional coupling overcomes this limit as only complex flow areas are solved with the 2D SWE. Elsewhere, where the flow is one-dimensional, this solution makes the most of long-time expertise in 1D model setting and calibration.

The present study focuses on multi-dimensional coupling in the context of real-time flood forecasting. The 1D SWE-based network model is widely used in hydraulics due to its relatively low computational cost. For such model the data assimilation (DA) capability has been already developed and used for flood forecasting, see Ricci et al. (2011). We demonstrate how the performance of the network model is improved by using the 2D-SWE based model locally, i.e. around a confluence point or across the flood plain area. Multi-dimensional coupling strategies in the field of hydrodynamics were proposed recently with heterogeneity in the complexity of the physics and the dimensions. An overlapping coupling strategy between 1D and 2D SWE models was proposed by Gejadze and Monnier (2007). They implemented a coupling strategy based on the conservation of the characteristic variables entering the 2D model and the injection of a lateral source term in the 1D model that is computed from the 2D model in a

\* Corresponding author.

E-mail address: [barthelemy@cerfacs.fr](mailto:barthelemy@cerfacs.fr) (S. Barthélémy).<sup>1</sup> Present address: 42 Avenue Gaspard Coriolis 31057 Toulouse Cedex 01, France.

flooding phase. This strategy was combined with variational DA and led to improved simulated results for academic test cases. Another strategy consists of coupling models at the lateral or longitudinal interfaces, without overlapping. Goutal et al. (2014) introduces a lateral coupling method between the 1D and 2D SWE models, describing the river flow in the main channel and over the flood plain, respectively, by considering variables between the 1D and 2D models as boundary fluxes for the 2D model and source terms for the 1D model. This strategy is based on successive resolutions of the 2D Riemann problem at the coupling interfaces and requires the estimation of the transverse velocity at the interfaces. The precision and efficiency of the method were illustrated with academic test cases. Based on Steinebach et al. (2004), Miglio et al. (2005) proposed longitudinal coupling between 1D and 2D SWE models where the continuity of Riemann variables across 1D/2D boundaries is preserved using the iterative Schwarz algorithm. This coupling is denoted by longitudinal as the interface is located at the upstream and downstream interfaces of 1D and 2D models, along the flow of the river. In another example of longitudinal coupling, Chen et al. (2012) proposed a new method based on the theory of characteristics to couple numerical models: the water-stage prediction-correction method. The approach of Miglio was re-visited and implemented with the coupling platform OpenPALM by Malleron et al. (2011). It was tested for a flood event on the Rhine river, and the water level difference between 1D/2D coupling and a full 2D model remain below 1%. Following this work, Tayachi (2013) and Blayo et al. (2017) developed a Schwarz algorithm for coupling the 1D SWE with the Navier-Stokes equations. The convergence properties of the global-time Schwarz (waveform) relation method have been studied for different partial differential equations, see e.g. (Gander and Stuart, 1998; Gander et al., 2003). The influence of the interface position between 1D and 2D models was highlighted. The ideas of this work were further developed by Daou et al. (2014) for 1D/3D coupling for monophasic/monophasic flow and monophasic/diphase flow. It was implemented on a real applicative case for inflow and outflow at a hydroelectric plant.

Following Malleron et al. (2011), the present study aims to develop an operational model of the Adour catchment in collaboration with SPC GAD (Service de Prévision des Crues Garonne-Adour-Dordogne) and SCHAPI (Service Central d'Hydrométéorologie et d'Appui la Prévision des Inondations). A 1D/2D longitudinal coupling strategy is proposed in the Adour catchment at the confluence between the Nive and the Adour rivers in Bayonne. The river network under consideration is divided into 3 parts: the upstream Nive (NU), the upstream Adour (AU) and the downstream Adour (AD). For each part the separate 1D sub-model is used, whereas the 2D model is created for the confluence area at Bayonne. As in Malleron et al. (2011) and Miglio et al. (2005), the iterative Schwarz algorithm is applied to preserve the continuity of hydraulic variables at the 1D/2D interfaces where the boundary conditions for each model are defined. An innovative feature of this work is that a DA filtering algorithm is applied over the 1D sub-models that are coupled to the 2D model.

The structure of the paper is as follows: Section 2 presents the 1D and 2D SWE formulations and the model set-up for the Adour Maritime and Bayonne area. The coupling strategy is described in Section 3 along with the DA algorithm for the 1D model. The details of the implementation of the coupling-DA strategy are also described. Results concerning the convergence and the computational cost of the coupling algorithm are presented in Section 4.1 and Section 4.2, respectively. The merits of the DA-coupling strategy for flood-forecasting are evaluated for a set of flood events and illustrated in Section 4.3. Conclusions of the study and future work are described in Section 5.

## 2. Modeling the hydrodynamics of the Adour river

### 2.1. The hydraulic solvers

The hydraulics numerical solvers MASCARET (Goutal and Maurel,

2002) and TELEMAC (Hervouet, 2007) are used in this study. These software were developed in the framework of the TELEMAC-MASCARET consortium (<http://www.opentelemac.org>). They are commonly used for simulations of dam-break wave, reservoir flushing and flooding.

#### 2.1.1. The 1D hydraulic model MASCARET

The one-dimensional SWE are written in terms of discharge  $Q$  [ $\text{m}^3\text{s}^{-1}$ ] and wet cross-section area  $A$  [ $\text{m}^2$ ] that relates to the water level  $h$  [m]. In a 1D model, the stream channel is described by a hydraulic axis corresponding to the main direction of the flow (the curvilinear abscissa denoted by  $s$  in [m]). The non-conservative form of the one-dimensional SWE (Goutal, 2014; Thual, 2010):

$$\begin{cases} \partial_t A(h) + \partial_s Q = 0 \\ \partial_t Q + \partial_s (Q(h)^2/A(h)) + gA(h)\partial_s h - gA(h)(S_0 - S_f) = 0 \end{cases} \quad (1)$$

with  $g$  [ $\text{m s}^{-2}$ ] the gravitational constant,  $S_0$  [–] the channel slope and  $S_f$  [–] the friction slope. These equations are usually combined with an equation for the friction slope  $S_f$ , here defined by the Manning-Strickler formula:

$$S_f = \frac{Q^2}{K_s^2 A(h)^2 R(h)^{4/3}}, \quad (2)$$

where  $R(h) = A(h)/P(h)$  is the hydraulic radius in [m] written as the ratio of the wet cross-section area  $A$  and the wet perimeter  $P(h)$  [m].  $K_s$  is the Strickler friction coefficient in [ $\text{m}^{1/3}\text{s}^{-1}$ ]. The hydraulic model requires the following input data: bathymetry, upstream and downstream boundary conditions, lateral inflows, roughness coefficients (specified over homogeneous zones) and initial conditions for the hydraulic state.

#### 2.1.2. The 2D hydraulic model TELEMAC

The 2D SWE are written in terms of the water depth  $h$  and the horizontal components of velocity,  $u$  and  $v$  [ $\text{m s}^{-1}$ ]:

$$\begin{aligned} \frac{\partial h}{\partial t} + \frac{\partial(hu)}{\partial x} + \frac{\partial(hv)}{\partial y} &= 0 \\ \frac{\partial(hu)}{\partial t} + \frac{u\partial(hu)}{\partial x} + \frac{v\partial(hu)}{\partial y} &= -gh\frac{\partial Z_s}{\partial x} - \frac{1}{K_s^2} \frac{gu\sqrt{u^2 + v^2}}{h^{1/3}} \end{aligned} \quad (3)$$

$$\frac{\partial(hv)}{\partial t} + \frac{u\partial(hv)}{\partial x} + \frac{v\partial(hv)}{\partial y} = -gh\frac{\partial Z_s}{\partial y} - \frac{1}{K_s^2} \frac{gv\sqrt{u^2 + v^2}}{h^{1/3}} \quad (4)$$

where  $K_s$  [ $\text{m}^{1/3}\text{s}^{-1}$ ] is the river bed and flood plain Strickler friction coefficient.  $Z_s$  [m] is the water free surface elevation ( $h = Z_s - Z_f$  where  $Z_f$  [m] is the bottom level described by the bathymetry and topography) and  $\nu_e$  [ $\text{m}^2\text{s}^{-1}$ ] is the water diffusion coefficient. To solve Eqs. (3) and (4), initial conditions  $h(x,y,t=0) = h_0(x,y)$ ;  $u(x,y,t=0) = u_0(x,y)$ ;  $v(x,y,t=0) = v_0(x,y)$  are provided, as well as with boundary conditions at the surface, at the bottom and at the upstream and downstream frontiers  $h(x_{BC}, y_{BC}, t) = h_{BC}(t)$ .

A two-dimensional area is described by a set of elements (triangular, with TELEMAC-2D), whose nodes are assigned a bathymetric value. In a 2D model, the geometrical representation of the river differs from the 1D modeling: there is no distinction between the main channel and the floodplain. The friction coefficient is defined over homogeneous zones on this mesh.

### 2.2. The hydraulic models for the Adour Maritime and Bayonne areas

The Adour Maritime 1D hydraulic model (AM) displayed in Fig. 1 covers about 160 km; it was set up for operational flood forecasting at SCHAPI and SPC GAD. It is composed of 7 reaches with 3 confluences between reaches 2 and 3, 4 and 5, and 6 and 7. There are 5 water-level observing stations along the network at Peyrehorade, Urt, Lesseps, Pont-Blanc and Villefranque. The upstream forcings at Dax, Orthez, Escos and Cambo are given by discharges computed from observed

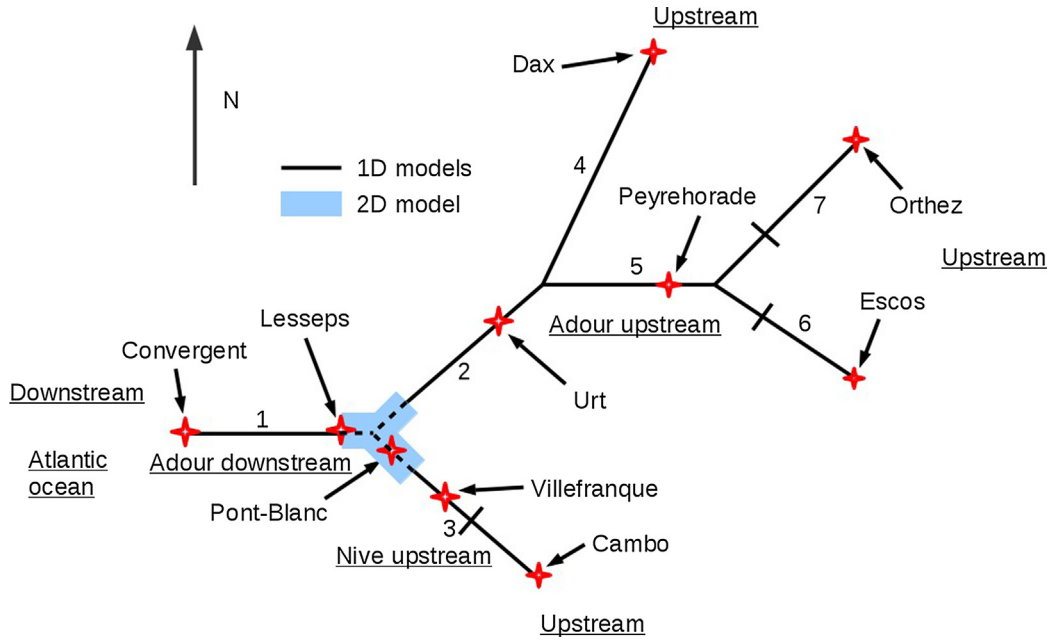


Fig. 1. Adour Maritime hydraulic modeling: local 2D model, full 1D model, 1D sub-models (Adour Upstream, Adour Downstream, Nive Upstream) and Bayonne 2D model. Numbers indicate the reaches, water level observing stations are represented by red crosses. Dams on reaches 3, 6 and 7 are represented by black markers.

water levels translated into discharge with local rating curves. In forecast mode, these forcing are defined constant, using the last observed value. The downstream forcing, at Convergent, is given by water level observations or forecasts. The entire network is under tidal influence except upstream of the dams located on reaches 3, 6 and 7. The full 1D model is composed of 2247 grid points. The Adour network is under maritime tidal influence combined with wet meteorological conditions due to water mass and heat flux exchanges with the ocean. It thus displays highly non linear dynamics. The Adour maritime area is thus one of the most sensitive zones to flooding risks, with a largest number of medium and maximum alerts raised by the flood forecasting services. Flood events on the Adour maritime network are characterized by sudden flood peaks along reaches 3, 6 and 7 that can occur simultaneously and last from 2 to 4 days. Flood events in reach 4 are characterized by long water-level rising periods (up to 9 days) and a slow water-level decreases (4 to 9 days). The AM hydraulic model was created from 548 bathymetric surveys throughout the network. The friction coefficient is defined in 20 areas and was calibrated to fit high tide water levels during past events.

The AM model was decomposed in three 1D sub-models that are coupled to a local 2D model (colored area) over the Bayonne area, as presented in Fig. 1:

- the Adour Upstream (AU) sub-model, which includes the Adour river upstream of the Bayonne area. It is composed of 5 reaches with 2 confluences and 2034 nodes.
- the Adour Downstream (AD) sub-model from Lesseps (downstream of the Bayonne area) to Convergent. It is composed of one reach with 95 nodes.
- the Nive upstream (NU) sub-model, which includes the Nive river upstream of the Garonne area. It is composed of 1 reach with 404 nodes.

The city of Bayonne is located on the banks of the Adour river at the confluence between the Adour and the Nive (confluence of reaches 1, 2 and 3 in Fig. 1). This highly urbanized area is threatened by flood events on the Nive river. In this area the flow is tidally influenced and during flood events the Nive river flows into the Plaine d'Ansot and the Barthe de Quartier Bas: the flow adopts a non-linear 2D dynamic

recirculation. For that reason, a 2D model for the Bayonne area where the Nive and the Adour rivers meet (Fig. 3-a) has been developed jointly by the SCHAPI and the SPC GAD for operational purposes. Upstream of Bayonne, for the Adour river, the 2D model starts at the highway A63 where the flow is mono-dimensionnal and the dikes stem the flow. For the Nive river, the 2D area includes the Plaine d'Ansot and the Barthe de Quartier Bas flood plains that stock and drain water during flood events on the Nive river. The 2D area includes Saint-Esprit, Petit Bayonne and Grand Bayonne at the Nive/Adour confluence; it ends at the Lesseps bridge downstream of Bayonne. In the present study, the observations at Lesseps are not assimilated, and the dynamics are driven by the maritime forcing at Convergent, about 5 km farther downstream. The 2D model with TELEMAC is composed of 33748 nodes and 66982 element.

### 3. Numerical methods

#### 3.1. Coupling algorithm between the 1D and 2D hydraulic models

The coupling algorithm used in this study is the multiplicative form of the global-in-time Schwarz algorithm adapted to the hydraulic case (Miglio et al., 2005; Malleron et al., 2011). In the present work, the upstream boundary conditions of the 1D models are prescribed by the discharge, and the downstream boundary conditions are prescribed by a wet surface. The upstream boundary conditions of the 2D model are prescribed by velocity vectors, while the 2D downstream boundary condition is prescribed by the water level. The multiplicative form of the global-in-time Schwarz algorithm applied to the AM-Bayonne area consists in solving the sub-problems in Eqs. (5) and (6), until the stopping criteria is verified:

$$\begin{cases} \mathcal{L}_1(A^k, Q^k) = 0 & \text{on } \Omega_{1D,i} \times [t; t + T], i = 1, 2, 3 \\ A_i^k = R_{21}(Z_{2D,i}^{k-1}) & \text{on } \Gamma_i \times [t; t + T], i = 1, 2 \\ Q_3^k = S_{21}((u^{k-1}, v^{k-1})_{2D,3}) & \text{on } \Gamma_3 \times [t; t + T] \end{cases} \quad (5)$$

$$\begin{cases} \mathcal{L}_2(h^k, u^k, v^k) = 0 & \text{on } \Omega_{2D} \times [t; t + T] \\ (u^k, v^k)_i = S_{12}(Q_{1D,i}^k) & \text{on } \Gamma_i \times [t; t + T], i = 1, 2 \\ h_{2D,3}^k = R_{12}(A_3^k) & \text{on } \Gamma_3 \times [t; t + T] \end{cases} \quad (6)$$

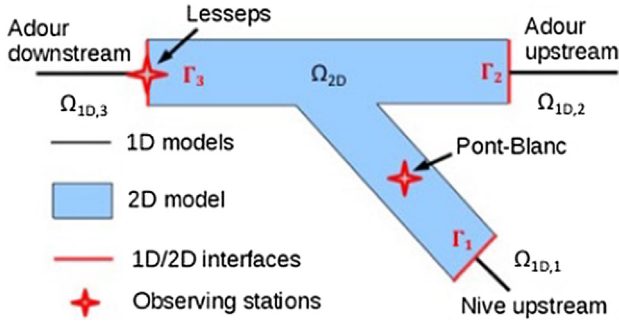


Fig. 2. Schematic representation of the relative placement of the 1D models compared to the 2D model and the coupling interfaces.

where  $\mathcal{L}_1$  and  $\mathcal{L}_2$  stand for the shallow-water operators for the 1D and the 2D models, respectively and  $\Omega_{2D}$  and  $\Omega_{1D,i}$  (with  $i = 1, 2, 3$ ), correspond to the 2D domain and the three 1D sub-domains, respectively represented in Fig. 2.  $\Gamma_i$  (with  $i = 1, 2, 3$ ) is the three 2D liquid boundaries,  $Z_{2D,i}^{k-1}$  is the mean 2D water level at the liquid boundary  $i$  (with  $i = 1, 2$ ). The boundary condition operators  $R_{21}, R_{12}, S_{21}$  and  $S_{12}$  are applied following the  $(x', y')$  local axis along and perpendicular to the flow and they are described as follows:

- $R_{21}$  translates the 2D water level along the cross-sectional interface  $\Gamma$  into a wet cross-sectional area for the 1D boundary condition. The 2D river width  $w(z)$  is integrated along the vertical axis  $z$  from the bottom of the river  $Z_f$  to the surface level  $Z_s$  for elements in the 1D/2D interface cross-section following  $y'$ :  $R_{21} = \int_{Z_f}^{Z_s} w(z) dz$ .
- $R_{12}$  translates the 1D wet cross-sectional area into the 2D water level along the wet cross-section following  $y'$ . If  $S$  and  $Z_s$  denote the wet cross-sectional area and the water free surface elevation then  $Z_s$  verify:  $S = \int_{Z_f}^{Z_s} w(z) dz$ . Hence the free surface elevation and the bathymetry at the coupling interface enable to compute the 2D water level to impose at the coupling interface;
- $S_{21}$  translates the velocity field at the 2D boundary  $\Gamma$  into a discharge that is imposed at the 1D boundary. The 2D water depth  $h_{2D}$  is multiplied by the velocity at each point along the cross-sectional area described by  $y'$ , then projected onto the local vector normal to the flow  $x'$  to compute the 1D discharge  $Q = \int_{\Gamma} h_{2D}(y') \cdot (u, v) \cdot \vec{n} dy'$ , where  $\vec{n}$  is the local normal vector to the 2D flow along  $x'$  and  $\cdot$  stands for the cross-product.
- $S_{12}$  translates the 1D discharge into 2D velocity components along  $y'$ . The 1D water level is mapped onto the 2D interface to compute the 2D water depth  $h_{2D}$ . Velocity vectors are derive from a parabolic profile proportional to  $\sqrt{h_{2D}}$ :  $u(x) = \alpha \sqrt{h(x)} \cdot n_{x'}$  and  $v(x) = \alpha \sqrt{h(x)} \cdot n_{y'}$ . The proportionality coefficient  $\alpha$  is set to ensure the discharge continuity at the 1D/2D interface  $-\int_{\Gamma} h(y') \cdot (u(y'), v(y')) \cdot \vec{n} dy' = Q$ .

At coupling iteration  $k$ , the boundary conditions applied at the interface of the 1D model for integration over  $[t; t + T]$  are prescribed from the results of the 2D model at iteration  $k-1$  over  $[t; t + T]$ . Once the 1D integration is completed the 2D boundary conditions for iteration  $k$  are prescribed from the results of the 1D model for integration over  $[t; t + T]$ . The iterative coupling strategy is applied sequentially in time over the length of the entire flood event.

Setting the stopping criteria requires a compromise between precision and computational time. Here, it is based on the continuity of the discharge and the water level at the interface, which implies the continuity of the Riemann invariant at the interface. This condition is necessary with respect to the hyperbolicity of each sub-problem for sub-critical flow. This formulation differs from that of Miglio et al. (2005), which ensures the continuity of wet cross-sectional area, discharge, and characteristic entering at the 1D/2D interface.

Following the conclusions of Tayachi (2013), it was verified that the flow remains mono-dimensional at the coupling interfaces, even for high flow rates. Velocity vectors at the 1D/2D interface ( $\Gamma_i, \Omega_{1D,i}$  from Fig. 2) from the 2D model are shown in Fig. 3-b (bottom-left of the plot). These vectors follow the 1D river center line for all simulation time steps (only one time is shown), ensuring that the coupling algorithm converges within a limited number of iterations.

### 3.2. Data assimilation algorithms in the 1D model

Several sources of uncertainty are identified in the hydraulic modeling. Hydrological forcing data, which describe the boundary conditions, usually result from the transformation of uncertain observed water levels into discharges through an uncertain rating curve or from discharges that are forecast by uncertain hydrological models. Additionally, the description of the river channel and flood plain geometry relies on a limited number of *in situ* measurements of topographic and bathymetric profiles that are then spatially interpolated. The simplification of the flow to a 1D representation is also a significant limitation. Finally, the calibration of friction coefficients is a pragmatic way to account for a variety of sources of uncertainty. Globally speaking, uncertainties in the input data and in the hydraulic parameters translate into uncertainties in the simulated hydraulic state. These uncertainties can be reduced with a DA algorithm that consists in combining water level (or discharge) *in situ* observations in the numerical model to correct the model forcing, parameters and/or state (Ricci et al., 2011; Habert et al., 2016; Madsen and Skotner, 2005). In the present case of 1D/2D coupling, improving the hydraulic state in the 1D sub-models results in improving the boundary conditions for the 2D model.

While ensemble data assimilation algorithms showed promising results for hydraulics and flood forecasting (e.g. Barthélémy et al., 2017), such algorithms were not considered here because of the computational cost. Instead the invariant Kalman Filter (IKF) from Ricci et al. (2011) was implemented. In this formulation, a simplified version of the Kalman Filter (Kalman, 1960) is implemented with the background error covariance matrix in Eq. 7, which is not propagated between assimilation cycles (to avoid either propagating an ensemble, or using the model tangent linear matrix and carrying our computationally expensive matrix multiplication). The analysis and propagation steps of the analysis are:

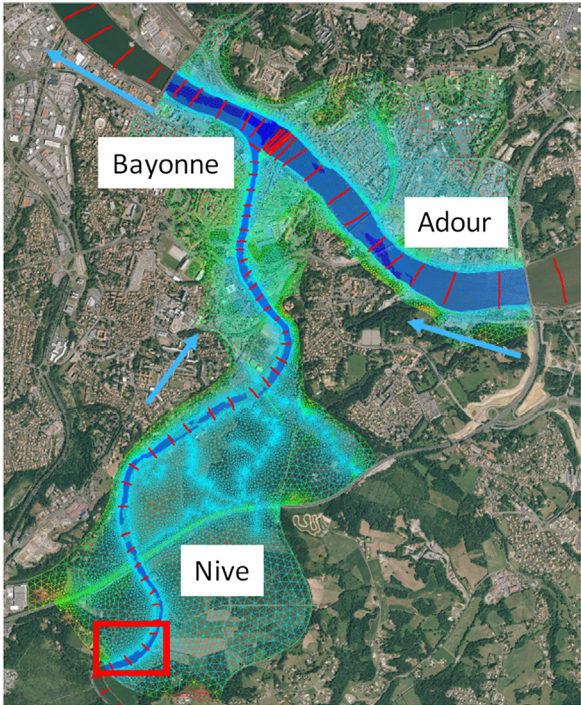
$$\begin{aligned} \mathbf{x}_i^a &= \mathbf{x}_i^b + \mathbf{B}\mathbf{H}^T(\mathbf{H}\mathbf{B}\mathbf{H}^T + \mathbf{R})^{-1}(\mathbf{Y}_i^o - \mathcal{H}(\mathbf{x}_i^b)) \\ \mathbf{x}_{i+1}^b &= \mathcal{M}_{i,i+1}(\mathbf{x}_i^a). \end{aligned} \quad (7)$$

where the control vector  $\mathbf{x} = (A, Q)$  corresponds to the discretized hydraulic state (excluding boundary values).  $\mathbf{x}_i^b$  and  $\mathbf{x}_i^a$  are respectively the background and analysis vector at time  $i$ ,  $\mathbf{B}$  is the background error covariance matrix,  $\mathbf{R}$  is the observation error covariance matrix,  $\mathbf{Y}_i^o$  is the observation vector at time  $i$ , and  $\mathcal{H}$  is the observation operator. In this study, since the flow is sub-critical, the background error correlation function is assumed to be an asymmetric Gaussian function with shorter correlation length scale downstream than upstream, as illustrated in Fig. 4. Further details about the DA algorithm and the results for the AM network are given in Ricci et al. (2011). In the 1D/2D coupling method, the DA analysis is applied at each observation time in each 1D sub-model; the analyzed state is then propagated in time by the 1D sub-models and exchanged with the 2D model interfaces.

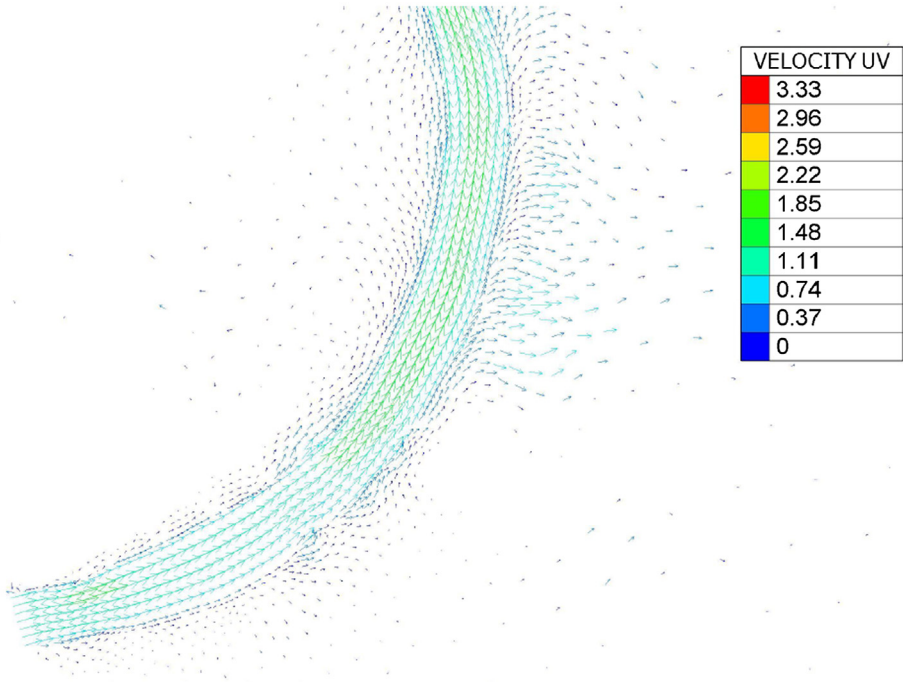
### 3.3. Cycled implementation of the coupling with OpenPALM

The DA algorithm is implemented with OpenPALM ([http://www.cerfacs.fr/globc/PALM\\_WEB/](http://www.cerfacs.fr/globc/PALM_WEB/)), (Piacentini et al., 2011). It is an open-source, flexible and powerful dynamic code coupler that has been developed jointly by CERFACS (Centre Européen de Recherche et Formation Avancée en Calcul Scientifique) and ONERA (Office National





(a)



(b)

**Fig. 3.** (a) 2D mesh over the Nive/Adour confluence. The red rectangle indicates the zoom area for panel (b), (b) Velocity field [ $\text{m s}^{-1}$ ] simulated by the 2D model on the Nive near the 1D/2D interface.

d'Etudes et de Recherches Aéronautiques) since 1998. OpenPALM was originally designed for DA algorithms in operational oceanography forecasting; it has now reached a high-degree of maturity and stability, with applications ranging from operational DA (oceanography, atmospheric chemistry, hydrology) to industrially-oriented multi-physics modeling (fluid-structure interactions, combustion-acoustics interactions). OpenPALM provides a straightforward parallel environment

based on high performance implementation of the Message Passing Interface (MPI) standard (i.e. MPICH, OpenMPI, LAM/MPI). This interface is able to perform both data parallelism (i.e. simultaneous execution on multiple cores of the same code for a unique data set with domain decomposition) and task parallelism (i.e. simultaneous execution on multiples cores of multiple tasks for the same or different data sets).

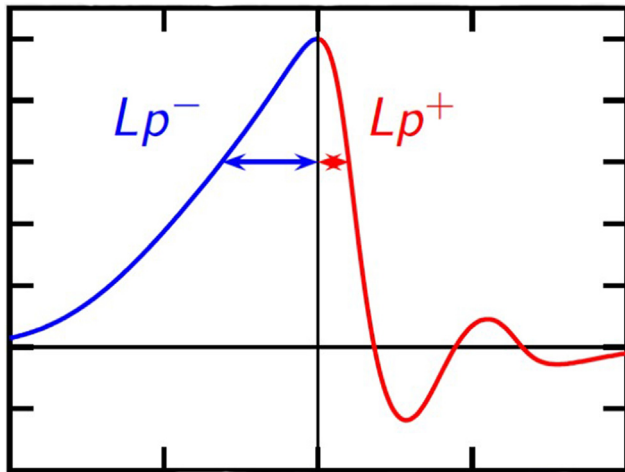


Fig. 4. Asymmetric Gaussian function with smaller correlation length scale downstream ( $L_p^+$ ) than upstream ( $L_p^-$ )

The OpenPALM coupling strategy relies both on task parallelism and data parallelism. The 2D model is executed on several processors (data parallelism) while in parallel (task parallelism) the 1D sub-models are

executed, each one, on different processors. The number of 1D sub-models and the number of processors to run the 2D model are user-defined and are handled by the OpenPALM coupling implementation so that this is generic for the user and can be applied to any hydraulic network. The Schwarz algorithm is implemented in 3 steps: initialization, iterative (over time) loops and finalization. The initialization step consists in reading the user-defined parameters, model parameters and geometries. These variables are allocated and stored in the OpenPALM block structure shared memory. These input variables, as well as the simulated wet area, discharge, and flow velocities at the 1D/2D interfaces are available for TELEMAC and MASCARET within the block structure. The data exchanges are achieved with OpenPALM communications. The finalization step consists in deallocating the variables. It should be noted that the stationary hypothesis for the KF algorithm implies that the cost of DA is limited to the matrix-vector product in Eq. (7), and thus represents a non-significant additional cost for the coupling algorithm. Still, when an observation is assimilated in the 1D model, a discontinuity with the 2D model may occur, and several iterations of the Schwarz algorithm may then be necessary to reconcile 1D and 2D models. The coupling/DA strategy is applied over a sliding time window that covers the coupled propagation of the dynamics and analysis steps for DA and a forecast period over which the 1D and 2D models are also coupled.

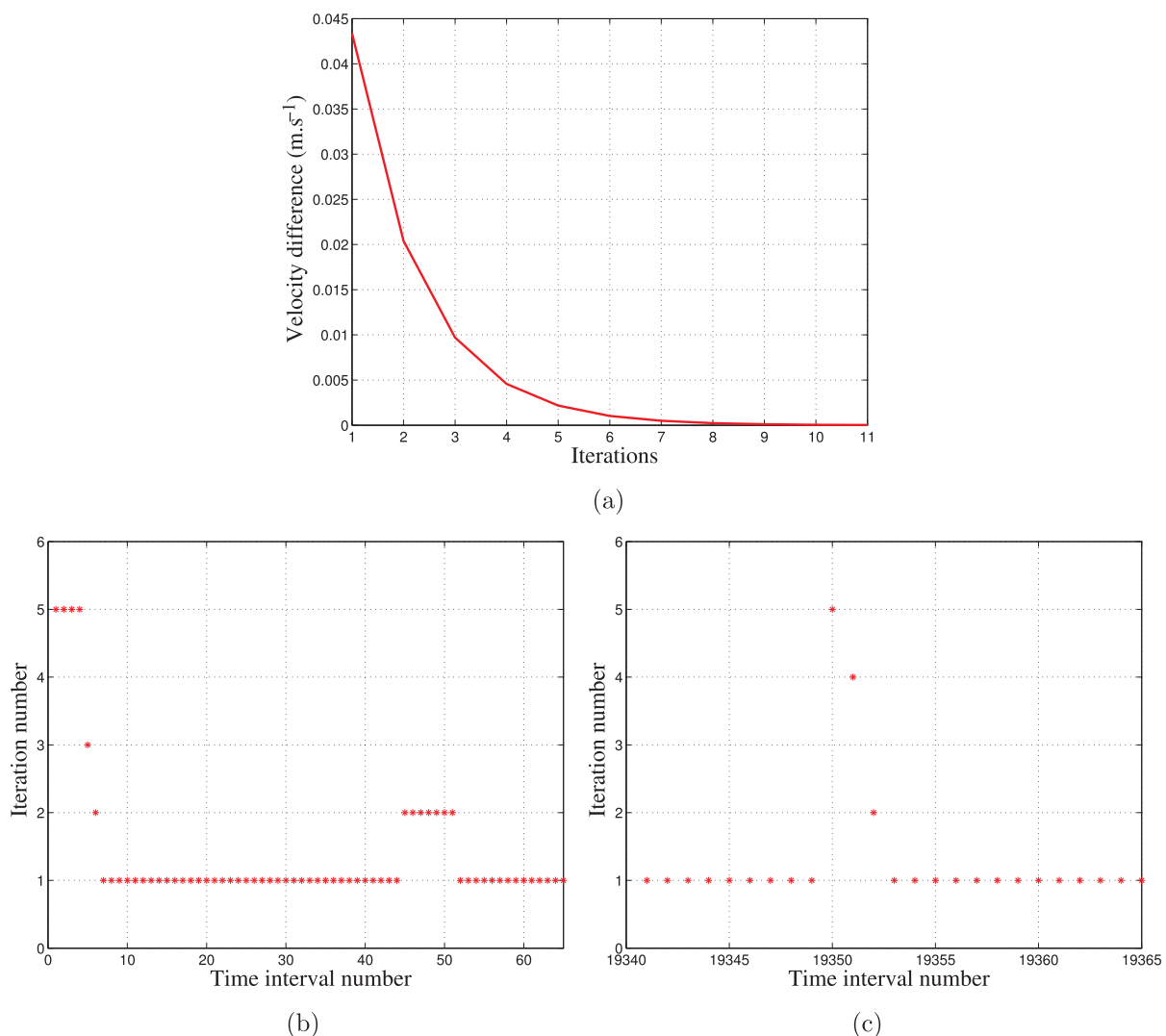


Fig. 5. (a) Convergence of the Schwarz algorithm, (b) Number of iterations for the Schwarz algorithm in the 1D/2D coupling, (c) Number of iterations for the Schwarz algorithm in the 1D/2D coupling with DA.

## 4. Results

### 4.1. Schwarz algorithm convergence

To the authors' knowledge, there are no theoretical results showing the Schwarz algorithm convergence in the case of multi-dimensional SWE. Yet, a convergence study was completed by Tayachi (2013) for a linearized 3D Navier-Stokes equations system coupled with a linearized 1D SWE system. It was shown that when absorbing boundary conditions are defined at the coupling interfaces, the Schwarz algorithm converges in 2 iterations. The convergence was studied in detail by Tayachi et al. (2014) for a toy model, and the importance of the interface position between the 1D and 2D models was confirmed: the coupling interface must be located in an area where there are no 2D effects, meaning that the flow is mono-dimensional. In the present work, the convergence study was carried out over a 2-day simulation period for a flood event in 2011. The stopping criteria was defined as a  $5.10^{-3}$  m difference between the 1D and 2D water levels and a  $0.01 \text{ ms}^{-1}$  difference in the velocities at the interface. The coupling time step is 8 s, which is also the 1D model time step, and the 2D model time step is 4 s.

Fig. 5-a displays the convergence of the velocity difference at the coupling interface as a function of the Schwartz iteration. This was calculated at the interface downstream of the 2D model. It was numerically observed (Fig. 5-b) that for the first coupling time steps, convergence usually occurs within a small number of iterations. For further coupling time-steps, convergence is reached after the first iteration. In all cases, the maximum number of iterations is set to 5 to limit the computational cost. When assimilation is performed, a discontinuity between the 1D and 2D models is introduced, and the convergence of the Schwarz algorithm may require more than one iteration as illustrated in Fig. 5-c. It should be noted that depending on the location of the 1D/2D interface, as well as the choice of the continuity variable, the convergence may be harder to reach. Yet the computational cost for 8 s of the 2D model simulation is not significant, and the cost of additional iterations for a small number of time steps has a negligible impact on the overall cost of the coupling over a flood event.

### 4.2. Optimal computational resources for coupled model

For the Bayonne 1D/2D coupled model, numerical coupling experiments with increasing numbers of processors were carried out on a High Performance Computing platform at CERFACS with 53 Tflop/s and 158 nodes with 2 Intel 8 cores processors Intel (SandyBridge 5.6 Ghz and 32Go of memory DDR3). Fig. 6 shows the accelerating factor, which is the cost of the model running on several processors compared to the cost of the model running on only one processor, for the local 2D model (red curve) and the coupled model (blue curve). The accelerating factor of the 2D model is smaller than the ideal accelerating factor (the black line that linearly depends on the number of processors used) and reaches a maximum of 15.8 for 32 processors (vertical, green dashed line). This is consistent with the general behavior of TELEMAC-2D, which is most efficient when approximately 1000 nodes are computed on each processor. The accelerating factor of the coupled model is also smaller than the ideal accelerating factor and than that of TELEMAC alone, reaching a maximum of 6.4 for 32 processors. This result is very important for operational flood forecasting services to calibrate their computational resources in order to run the 1D/2D multi-dimensional coupled model. It should be noted that in this comparison, the 2D model is local, while the coupled model covers the entire network with the 1D model. The loss of scalability is due to the multiplicative Schwarz algorithm in which the 2D model waits for the 1D model results at the current iteration  $k$ .

### 4.3. Coupling used in flood forecasting

The 1D/2D coupling/DA strategy was applied to model a set of 7

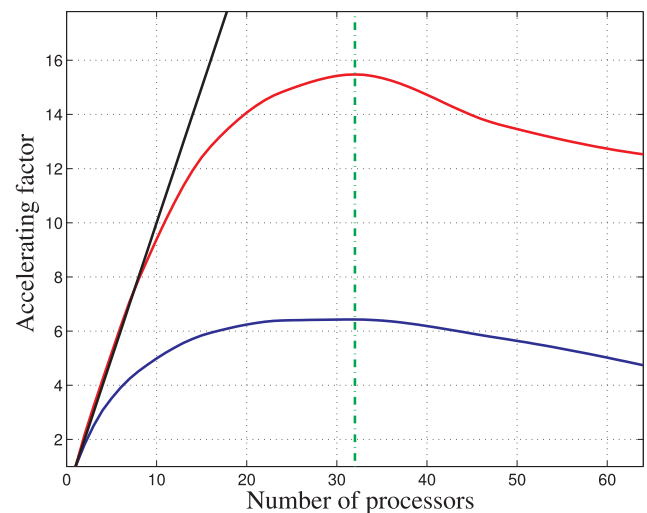


Fig. 6. Accelerating factor for the coupled model (blue line), ideal accelerating factor (black line) and stand alone TELEMAC model accelerating factor (red line). The optimal domain decomposition is reached for 32 processors (vertical dashed green line). (For interpretation of the references to colour in this figure legend, the reader is referred to the web version of this article.)

real flood events (with and without DA) in the AM catchment with hydrological data provided by the SPC GAD. The water level at the observing stations is displayed for the 2014 flood event in Fig. 7, except at Peyrehorade where the 2009 event is used (this event presents the most visible results). In each panel, the blue line represents the observations, the black line represents the full 1D AM model output, the green line represents the coupled model output without DA, and the red line represents the coupled model with DA.

For each flood event, the statistical results including the bias and Root Mean Square Error (RMSE) computed with respect to the observations, are presented in Fig. 8 and Fig. 9, respectively, for the analysis at 0 h lead time (solid lines) and for the forecast at the maximum lead time of each observing station (dashed lines). The 0 h lead time and the maximum lead time are respectively, the initial time of forecast and the transfer time of the upstream boundary condition beyond which a forecast can not be performed because upstream boundary conditions are set constant during the forecast period. The 1D model results are plotted in black, the coupled model without DA results are plotted in green, and the coupled model with DA results are plotted in red. The mean bias and RMSE computed over the 7 flood events are shown in Table 1.

#### 4.3.1. Coupled model without data assimilation

The merits of the 1D/2D coupling are described for the different observing stations.

**Pont-Blanc (2D area)** – The 2D model around Bayonne improves the simulated water level at Pont-Blanc compared to the 1D model, especially for high flow rates as illustrated in Fig. 7-a. For the 2014 event, the water level increases when using the coupling solution at low tide, and the shape of the limnigraph is improved for high flow events even though the water level remains slightly underestimated. The bias is reduced for all 7 flood events, as shown in Fig. 8-a, equivalently for the 0 h and maximum lead times, with a mean negative bias of  $-19 \text{ cm}$  for the 1D model reducing to  $-13 \text{ cm}$  for the coupled model (Table 1). The RMSE is also reduced for all events (Fig. 9-a), with a mean RMSE of  $0.25 \text{ cm}$  for the 1D model reducing to  $0.17 \text{ cm}$  for the coupled model, with smaller improvements as the lead time increases (Table 1).

**Villefranque (NU)** – The improvements observed in the 2D area, especially over the Plaine d'Ansot and the Barthe de Quartier Bas, also improves the boundary condition at the 1D/2D interface and consequently in the 1D section upstream of the interface on the Nive, as

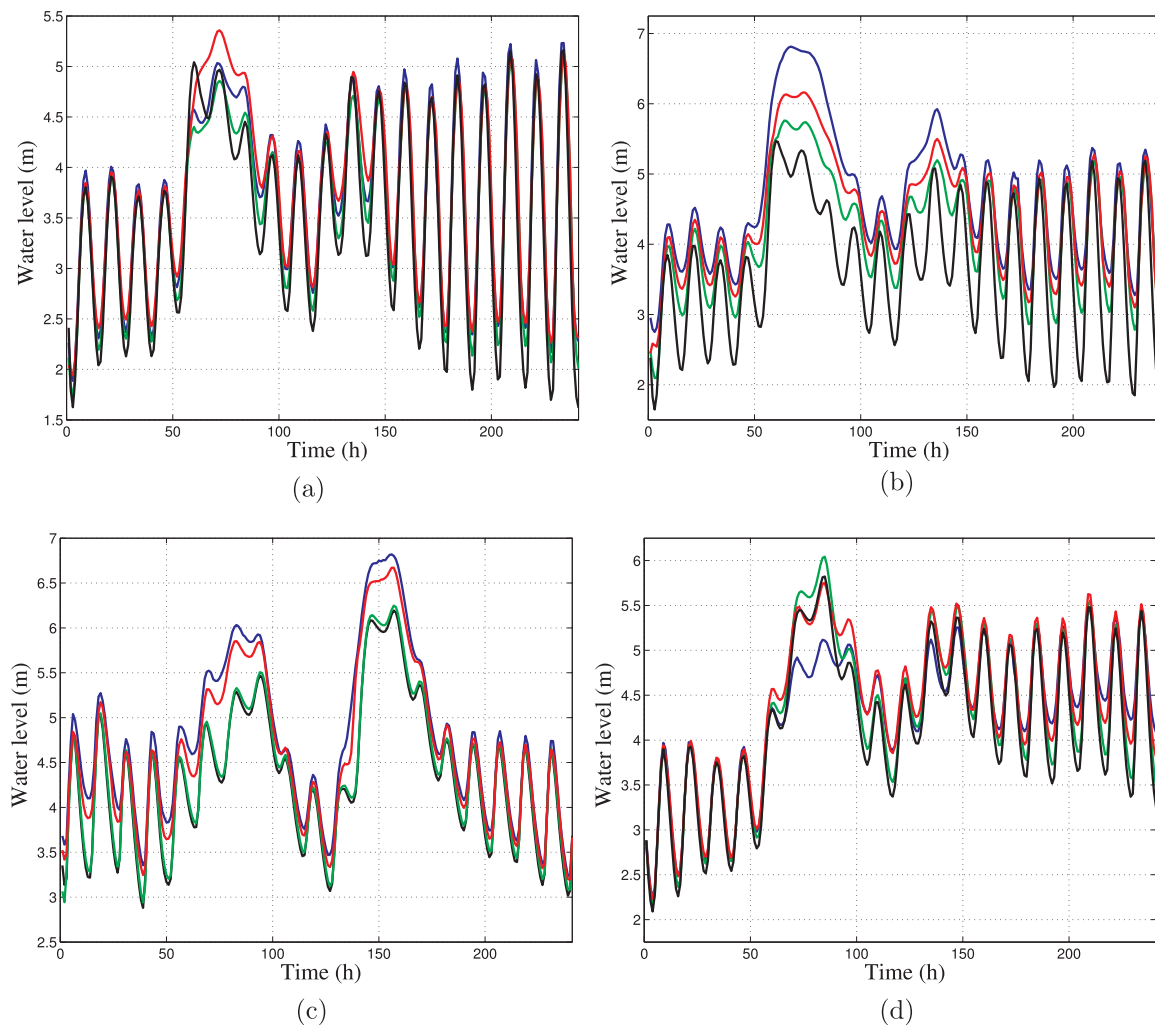


Fig. 7. Analyzed water level at (a) Pont Blanc, (b) Villefranche, (c) Peyrehorade and (d) Urt. The blue line represents the observations, the black line represents the 1D model, the green line represents the coupled model without DA and the red line represents the coupled model with DA.

illustrated in Fig. 7-b. For the 2014 event, the full 1D model strongly under estimates the water level, especially at high flow rates, and the coupling solution brings more water into the system. The bias is significantly reduced for all 7 flood events as shown in Fig. 8-b, -b, equivalently for the 0 h and maximum lead time, with a mean negative bias of  $-77$  cm reducing to  $-40$  cm (Table 1). The RMSE is also significantly reduced for all events (Fig. 9-b), with a RMSE of  $0.90$  cm for the 1D model reducing to  $0.46$  cm for the coupled model, with similar improvements as the lead time increases (Table 1).

**Peyrehorade (AU)** – The AU hydrodynamics is mono-dimensional, thus the impact of the coupling with respect to the 1D model is limited at Peyrehorade, as shown in Fig. 7-c. At Peyrehorade, which is far from the 2D area, the improvement of the 1D/2D coupling is small for the 2009 event. The bias is slightly reduced for all 7 flood events as shown in Fig. 8-c, equivalently for the 0 h and maximum lead times, with a mean negative bias of  $-30$  cm reducing to  $-26$  cm (Table 1). The RMSE is reduced for all events (Fig. 9-c), with a mean RMSE of  $0.40$  cm for the AM 1D model reducing to  $0.35$  cm for the coupled model, with similar improvements as the lead time increases (Table 1).

**Urt (AU)** – At Urt, the water level is improved for medium flow rates (especially at low tide) but not for high flow rates as shown in Fig. 7-d. At this observing station, the 1D hypothesis is not valid, and the 2D flood plain modeling should be taken into account. For high flow rates, the 1D model tends to over estimate the water level. Since the coupling tends to add water into the system, it has a negative impact at high flow

rates at Urt. The time averaged bias decreased for some events and increased for others (Fig. 8-d). The RMSE results are not impacted by the coupling (Fig. 9-d and Table 1).

**Lesseps (AD)** – The impact of coupling at Lesseps is not visible neither in the bias nor on the RMSE, independent of the lead time (Figs. 8, 9-e, Table 1 as the dynamics are driven by the maritime boundary conditions).

#### 4.3.2. Coupled model with data assimilation

The merits of DA in the 1D model coupled to the 2D model are described here for the different observing stations.

**Pont-Blanc (2D area)** – Observations at Pont-Blanc are not assimilated as this observing station is located in the 2D area. The assimilation of observations at Villefranche, upstream of Pont-Blanc, tends to cause an over estimation of the water level at high flow rates for the 2014 event, as illustrated in Fig. 7-a. For the 7 flood events, it has a positive impact on the bias (Fig. 8-a), with a decrease of the mean bias from  $-13$  cm (for the coupled model) to less than  $1$  cm at 0 h and maximum lead times (Table 1). DA strongly reduces the bias with respect to the 1D model and the coupled simulation. Yet, as expected when correcting the model state, the merits of DA decrease as the lead time increases. The RMSE (Fig. 9-a) is slightly reduced by DA, but most of the RMSE improvements were already achieved with the coupling (Table 1).

**Villefranche (NU)** – The DA analysis has a significant effect at



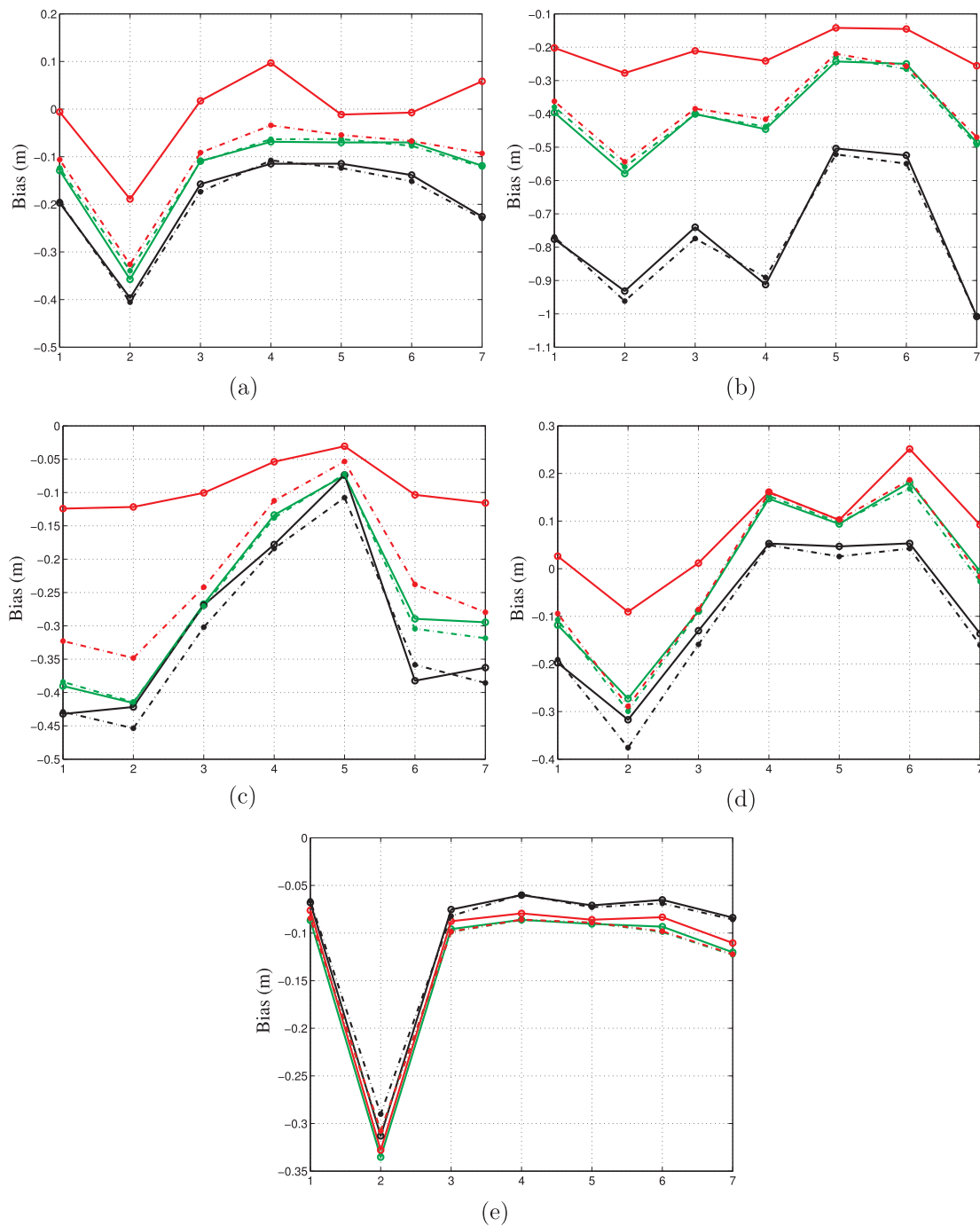


**Fig. 8.** Bias at (a) Pont Blanc, (b) Villefranche, (c) Peyrehorade, (d) Urt, (e) Lesseps computed with respect to the observations, for each flood event (numbered 1 to 7 in x-axis) at 0 h lead time (solid lines) and maximum lead time (dashed lines). The black lines represent the 1D model, the green lines represent the coupled model without DA and the red line represent the coupled model with DA. (For interpretation of the references to colour in this figure legend, the reader is referred to the web version of this article.)

Villefranche where the 1D model does not represent well the observations even taking into account the improvements gained by the coupling during the 2014 event and especially at high flow rates, as illustrated in Fig. 7-b. The assimilation reduces the negative bias from  $-77$  cm (for the 1D model) to  $-21$  cm at the 0 h lead time and  $-38$  cm at the maximum lead time (Table 1). The bias reduction is clearly visible in Fig. 8-b, -b, with a reduced impact for a larger lead time. The RMSE is also significantly improved by DA for all flood events (Fig. 9-b). The mean RMSE is 25 cm at the 0 h lead time and 49 cm at the maximum lead time, compared to 90 cm for the 1D model (and 46 cm for the coupled model), as shown in Table 1.

**Peyrehorade (AU)** – At Peyrehorade, the model without DA provides poor results, especially during flood peaks. DA leads to a significant improvement in the simulated water level, as illustrated in Fig. 7-c for the 2009 flood event: the water level is increased. For the 7 flood events, the RMSE and bias are greatly improved with stronger impacts for shorter lead times as expected (Figs. 8-c and 9-c). The bias and RMSE are reduced on average to less than 10 cm and 12 cm (Table 1).

**Urt (AU)** – At Urt, DA has little impact on the results, and the simulated water level remains far from the observations, especially for high flow rates, as presented in Fig. 7-d. The 1D model is not able to

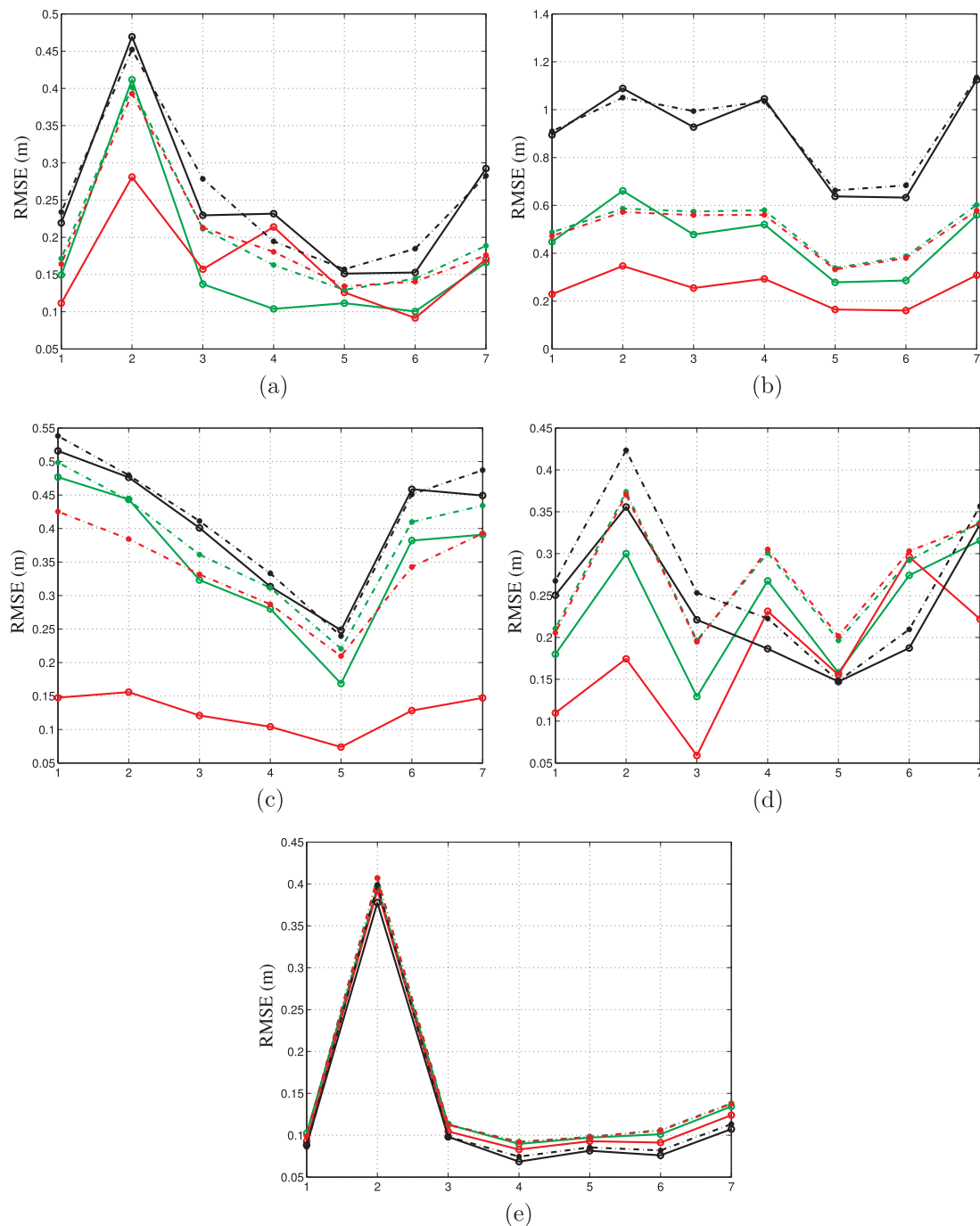


**Fig. 9.** RMSE at (a) Pont Blanc, (b) Villefranche, (c) Peyrehorade, (d) Urt, (e) Lesseps computed with respect to the observations, for each flood event (numbered 1 to 7 in x-axis) at 0 h lead time (solid lines) and maximum lead time (dashed lines). The black lines represent the 1D model, the green lines represent the coupled model without DA and the red line represent the coupled model with DA.

represent the flood plain dynamics and over-estimates water levels in spite of the assimilation of observations at Peyrehorade and Urt. In fact, the assimilation of observations at Peyrehorade may cause a degradation at Urt when the water is over-estimated at Urt and under estimated at Peyrehorade (or conversely). The 1D model bias was already small, but was further reduced by coupling, increasing a little due to DA and the RMSE of 20 cm did not change (Table 1).

**Lesseps (AD)** – Observations at Lesseps are not assimilated because this station is located at the coupling interface between the 2D model and the 1D model Adour Downstream. As previously noted for the coupling, DA has a negligible impact at Lesseps.

## 5. Conclusion

This study describes the application of a multi-dimensional coupling strategy between 1D and 2D models on the Adour maritime catchment, where the confluence between the Nive and the Adour rivers is simulated with a 2D local model, and the upstream and downstream parts of the rivers are simulated with 1D sub-models. The models are coupled at their longitudinal boundaries with an iterative Schwarz algorithm applied at each interface. A Kalman Filter data assimilation algorithm is also applied in the 1D models so that *in situ* water level observations are assimilated to correct the simulated and forecasted water level and discharge. The data assimilation and coupling strategy is implemented

**Table 1**  
Bias and RMSE computed with respect to the observations, averaged over the 7 flood events for the 1D model (1D), the coupled model without DA (C) and the coupled model with DA (CDA) at the 0 h lead time and the maximum lead time.

	Pont Blanc			Villefranche			Peyrehorade			Urt			Lesseps		
	1D	C	CDA	1D	C	CDA	1D	C	CDA	1D	C	CDA	1D	C	CDA
0 h lead time	−0.1921	−0.1319	−0.0058	−0.7709	−0.4002	−0.2106	−0.3028	−0.2665	−0.0929	−0.0899	−0.009	0.0793	−0.1052	−0.1297	−0.1215
Max lead time	−0.198	−0.1284	−0.1103	−0.7819	−0.3952	−0.3791	−0.3172	−0.2717	−0.228	−0.1098	−0.0151	−0.0052	−0.1036	−0.127	−0.1266
Mean RMSE (m)	Pont Blanc			Villefranche			Peyrehorade			Urt			Lesseps		
	1D	C	CDA	1D	C	CDA	1D	C	CDA	1D	C	CDA	1D	C	CDA
0 h lead time	0.2494	0.1685	0.1645	0.9072	0.4615	0.251	0.4089	0.3522	0.1254	0.2404	0.232	0.1782	0.1282	0.1477	0.1402
Max lead time	0.2548	0.2014	0.2002	0.9243	0.508	0.4935	0.4199	0.3826	0.3390	0.2687	0.2724	0.2737	0.134	0.1506	0.1501

with the OpenPALM dynamical coupling software that allows for an efficient management of task and data parallelism. The developed strategy is compatible with operational computational cost constraints. The strategy was applied to simulate a set of 7 flood events in the Adour catchment. It was shown that the coupling algorithm converges with at most 5 iterations, and the water level and velocity continuity is guaranteed at the model interfaces. Numerical experiments were performed on 32 processors to achieve the scalability skills of the 2D model of the local area. Further work is needed to determine more precise conclusions since a full 2D model is not yet available on the Adour area. The results highlighted that the coupling with the local 2D solution significantly improves the simulation in the 2D and 1D areas. Data assimilation in 1D sub-models also leads to significant improvements for simulations and for short term forecasts since only the model state is corrected. Yet, the improvements are minor in 1D areas where the 1D model results are not satisfying, for instance at Urt where flood plain modeling should be activated.

Future work includes the implementation of the additive scheme for the Schwarz algorithm, which should decrease the computational cost of the coupled strategy since the 1D and 2D models would then run in parallel for an iteration with no waiting delay. Preliminary work on this formulation presented convergence issues that require further investigation. Alternative coupling strategies are also being investigated. Lateral coupling between the 1D model of the river bed and the 2D model of the flood plains allows activating the 2D model only for high flow rates when the 1D model simulates overflows in the flood plains. This strategy remains compatible with data assimilation in the 1D model. Finally, efforts are being made to develop data assimilation for the 2D models for state and parameter corrections with an ensemble-based approach. This choice enables a flow-dependent estimation of the background error covariances. Keeping the cost of such ensemble-based algorithms compatible with operational computational constraints remains a key challenge. For that reason, the use of a surrogate model in place of the forward model should be envisaged.

## Acknowledgements

The authors acknowledge the SPC GAD for providing the observed and hydrological data. Funding for this study was provided by SCHAPI and the EoCoE (Energy Oriented Center of Excellence) H2020 European project WP4.

## References

- Barthelemy, S., Ricci, S., Rochoux, M.C., Le Pape, E., Thual, O., 2017. Ensemble-based data assimilation for operational flood forecasting – On the merits of state estimation for 1D hydrodynamic forecasting through the example of the Adour Maritime river. *J. Hydrol.* 552, 210–224.
- Blayo, E., Rousseau, A., Pigeonnat, M.T., 2017. Boundary conditions and Schwarz waveform relaxation method for linear viscous Shallow Water equations in hydrodynamics. *SMAI J. Comput. Math.* 3, 117–137.
- Chen, Y., Wang, Z., Liu, Z., Zhu, D., 2012. 1D–2D coupled numerical model for shallow-water flows. *J. Hydraulic Eng.* 138 (2), 122–132.
- Daou, M.P., Blayo, E., Rousseau, A., Bertrand, O., Pigeonnat, T., Coulet, C., Goutal, N., 2014. Coupling 3D Navier-Stokes and 1D shallow water models. *Simhydro 2014*, Jun 2014, Sophia Antipolis, France hal-00995171.
- Gander, M.J., Halpern, L., Nataf, F., 2003. Optimal schwarz waveform relaxation for the one dimensional wave equation. *SIAM J. Numer. Anal.* 41 (5), 1643–1681.
- Gander, M.J., Stuart, A.M., 1998. Space-time continuous analysis of waveform relaxation for the heat equation. *SIAM J. Sci. Comput.* 19 (6), 2014–2031.
- Gejadze, I.Y., Monnier, J., 2007. On a 2D 'zoom' for the 1D shallow water model: coupling and data assimilation. *Comput. Methods Appl. Mech. Eng.* 196 (45–48), 4628–4643.
- Goutal, N., 2014. Développements autour de la simulation des écoulements à surface libre en rivière. *Equations de Saint-Venant – Couplage de modèles - Incertitudes – Application aux ondes de submersion*. PhD thesis.
- Goutal, N., Maurel, F., 2002. A finite volume solver for 1D shallow-water equations applied to an actual river. *Int. J. Numer. Meth. Fluids* 38 (1), 1–19.
- Goutal, N., Parisot, M., Zaoui, F., 2014. A 2D reconstruction for the transverse coupling of shallow water models. *Numer. Methods Fluids* 75 (11), 775–799.
- Hubert, J., Ricci, S., Pape, E.L., Thual, O., Piacentini, A., Goutal, N., Rochoux, M., 2016. Reduction of the uncertainties in the water level-discharge relation of a 1D hydraulic model in the context of operational flood forecasting. *J. Hydrol.* 532, 52–64.

- Hervouet, J.-M., 2007. *Hydrodynamics of Free Surface Flows: Modelling with the Finite Element Method*. John Wiley & Sons.
- Kalman, R.E., 1960. A new approach to linear filtering and prediction problems. *J. Basic Eng.* 82 (1), 35–45.
- Madsen, H., Skotner, C., 2005. Adaptive state updating in real-time river flow forecasting – A combined filtering and error forecasting procedure. *J. Hydrol.* 308 (1–4), 302–312.
- Malleron, N., Zaoui, F., Goutal, N., Morel, T., 2011. On the use of a high-performance framework for efficient model coupling in hydroinformatics. *Environ. Modell. Softw.* 26 (12), 1747–1758.
- Miglio, E., Perotto, S., Saleri, F., 2005. Model coupling techniques for free-surface flow problems: Part i. *Nonlinear Anal.: Theory, Methods Appl.* 63 (5–7), e1885–e1896.
- Piacentini, A., Morel, T., Thévenin, A., Duchaine, F., 2011. O-Palm: An open source dynamic parallel coupler. In: *Proceedings of the 4th International Conference on Computational Methods for Coupled Problems in Science and Engineering, COUPLED PROBLEMS 2011*.
- Ricci, S., Piacentini, A., Thual, O., Pape, E.L., Jonville, G., 2011. Correction of upstream flow and hydraulic state with data assimilation in the context of flood forecasting. *Hydrol. Earth Syst. Sci.* 15 (11), 3555–3575.
- Steinebach, G., Rademacher, S., Rentrop, P., Schulz, M., 2004. Mechanisms of coupling in river flow simulation systems. *J. Comput. Appl. Math.* 168 (1–2), 459–470.
- Tayachi, M., 2013. *Couplage de modèles de dimensions hétérogènes et application en hydrodynamique*. PhD thesis.
- Tayachi, M., Rousseau, A., Blayo, E., Goutal, N., Martin, V., 2014. Design and analysis of a Schwarz coupling method for a dimensionally heterogeneous problem. *Int. J. Numer. Meth. Fluids* 75 (6), 446–465.
- Thual, O., 2010. *Hydrodynamique de l'environnement*. Ecole polytechnique.